Response Surface Methodology As a New Approach for Finding Optimal MALDI Matrix Spraying Parameters for Mass Spectrometry Imaging

Dušan Veličković, Guanshi Zhang, Dejan Bezbradica, Arunima Bhattacharjee, Ljiljana Paša-Tolić, Kumar Sharma, Theodore Alexandrov, Christopher R. Anderton,* and KPMP Consortium
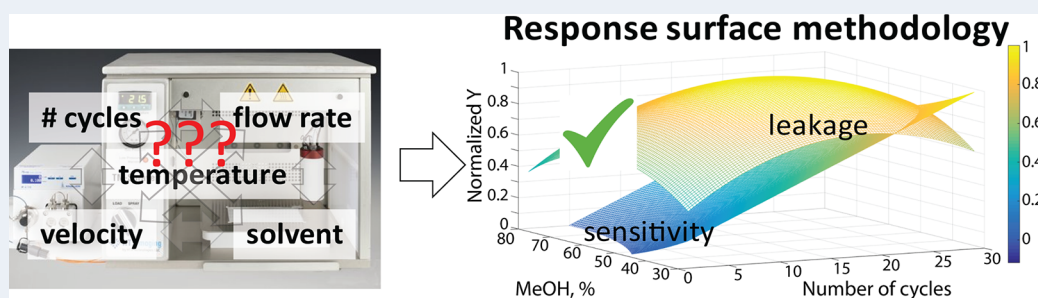
Read Online

ACCESS | Metrics & More | Article Recommendations | Supporting Information

ABSTRACT: Automated spraying devices have become ubiquitous in laboratories employing matrix-assisted laser desorption/ionization mass spectrometry imaging (MALDI-MSI), in part because they permit control of a number of matrix application parameters that can easily be reproduced for intra- and interlaboratory studies. Determining the optimal parameters for MALDI matrix application, such as temperature, flow rate, spraying velocity, number of spraying cycles, and solvent composition for matrix application, is critical for obtaining high-quality MALDI-MSI data. However, there are no established approaches for optimizing these multiple parameters simultaneously. Instead optimization is performed iteratively (i.e., one parameter at a time), which is time-consuming and can lead to overall nonoptimal settings. In this report, we demonstrate the use a novel experimental design and the response surface methodology to optimize five parameters of MALDI matrix application using a robotic sprayer. Thirty-two combinations of MALDI matrix spraying conditions were tested, which allowed us to elucidate relationships between each of the application parameters as determined by MALDI-MS (specifically, using a 15 T Fourier transform ion cyclotron resonance mass spectrometer). As such, we were able to determine the optimal automated spraying parameters that minimized signal delocalization and enabled high MALDI sensitivity. We envision this optimization strategy can be utilized for other matrix application approaches and MALDI-MSI analyses of other molecular classes and tissue types.

KEYWORDS: *experimental design, METASPACE, molecular annotation, delocalization quantification, human biopsy*

■ INTRODUCTION

Matrix-assisted laser desorption/ionization mass spectrometry imaging (MALDI-MSI) has emerged as a powerful tool to visualize the distribution of a wide range of molecules within biological samples.[1−5] MALDI-MSI relies on a crystallized layer of energy-absorbing matrix molecules over a sample. The MALDI matrix, usually a low molecular weight aromatic acid or base, both protects endogenous analytes from being degraded during the laser ablation and assists in ionization of endogenous analytes in the gas phase.[6] In MALDI-MSI, homogeneous matrix deposition is of the utmost importance in order to ensure that any detected structure or heterogeneity in an ion image reflects molecular content of the sample rather than matrix application or crystallization artifacts (e.g., "hot spots"). Additionally, analyte delocalization ("leakage"), which can be caused by the diffusion of endogenous compounds

inside the matrix solution prior to crystallization, should be minimized to retain the spatial-molecular features of the sample being analyzed.[7] Recently, Huizing et al.[7] demonstrated a method to measure delocalization of tissue molecules by considering a curve of intensities of pixels along a line crossing the edge of the tissue, and they used this approach to compare different MALDI matrix application methods.

MALDI matrix application is commonly performed via spraying with an airbrush, sublimation of the matrix onto the sample, or with an automated spraying device.[1] Airbrush

Table 1. Experimental Design, With Coded and (Actual) Values of Factors

|						factor	
	temp (°C)	flow rate (mL/min)	spraying velocity (mm/min)	cycles (number)	methanol conc (%)	co-localization with glomeruli (correlation value)	lipid annotations (no.)
expt	X1	X2	X3	X4	X5	Y1	Y2
1	1 (67.5)	1 (0.1525)	1 (1125)	1 (22)	1 (67.5)	0.191	164
2	1 (67.5)	1 (0.1525)	1 (1125)	−1 (8)	−1 (42.5)	0.321	159
3	1 (67.5)	1 (0.1525)	−1 (775)	1 (22)	−1 (42.5)	0.187	65
4	1 (67.5)	1 (0.1525)	−1 (775)	−1 (8)	1 (67.5)	0.277	191
5	1 (67.5)	−1 (0.0575)	1 (1125)	1 (22)	−1 (42.5)	0.517	333
6	1 (67.5)	−1 (0.0575)	1 (1125)	−1 (8)	1 (67.5)	0.464	98
7	1 (67.5)	−1 (0.0575)	−1 (775)	1 (22)	1 (67.5)	0.491	204
8	1 (67.5)	−1 (0.0575)	−1 (775)	−1 (8)	−1 (42.5)	0.542	226
9	−1 (42.5)	1 (0.1525)	1 (1125)	1 (22)	−1 (42.5)	0.124	142
10	−1 (42.5)	1 (0.1525)	1 (1125)	−1 (8)	1 (67.5)	0.151	213
11	−1 (42.5)	1 (0.1525)	−1 (775)	1 (22)	1 (67.5)	0.046	123
12	−1 (42.5)	1 (0.1525)	−1 (775)	−1 (8)	−1 (42.5)	0.347	120
13	−1 (42.5)	−1 (0.0575)	1 (1125)	1 (22)	1 (67.5)	0.467	324
14	−1 (42.5)	−1 (0.0575)	1 (1125)	−1 (8)	−1 (42.5)	0.363	218
15	−1 (42.5)	−1 (0.0575)	−1 (775)	1 (22)	−1 (42.5)	0.357	241
16	−1 (42.5)	−1 (0.0575)	−1 (775)	−1 (8)	1 (67.5)	0.325	167
17	2 (80)	0 (0.105)	0 (950)	0 (15)	0 (55)	0.521	113
18	−2 (30)	0 (0.105)	0 (950)	0 (15)	0 (55)	0.471	126
19	0 (55)	2 (0.2)	0 (950)	0 (15)	0 (55)	0.467	50
20	0 (55)	−2 (0.01)	0 (950)	0 (15)	0 (55)	0.306	123
21	0 (55)	0 (0.105)	2 (1300)	0 (15)	0 (55)	0.63	191
22	0 (55)	0 (0.105)	−2 (600)	0 (15)	0 (55)	0.488	106
23	0 (55)	0 (0.105)	0 (950)	2 (29)	0 (55)	0.121	214
24	0 (55)	0 (0.105)	0 (950)	−2 (1)	0 (55)	0.455	11
25	0 (55)	0 (0.105)	0 (950)	0 (15)	2 (80)	0.242	187
26	0 (55)	0 (0.105)	0 (950)	0 (15)	−2 (30)	0.399	129
27[a]	0 (55)	0 (0.105)	0 (950)	0 (15)	0 (55)	0.343	190
28[a]	0 (55)	0 (0.105)	0 (950)	0 (15)	0 (55)	0.318	132
29[a]	0 (55)	0 (0.105)	0 (950)	0 (15)	0 (55)	0.313	157
30[a]	0 (55)	0 (0.105)	0 (950)	0 (15)	0 (55)	0.463	126
31[a]	0 (55)	0 (0.105)	0 (950)	0 (15)	0 (55)	0.472	184
32[a]	0 (55)	0 (0.105)	0 (950)	0 (15)	0 (55)	0.399	139

[a]Central point.

matrix application is one of the original methods, which utilizes the spraying tools developed for thin-layer chromatography.[8,9] While this approach is relatively fast and simple, it has limited reproducibility due to the spray velocity and the flow rate being controlled manually. Matrix sublimation benefits from not requiring a solvent for application, which minimizes analyte delocalization and produces highly homogeneous matrix films, but at the cost of poor analyte extraction from the sample (to form cocrystals with the matrix) that leads to low sensitivity.[10,11] Recrystallization and automated methodologies are recent advancements in the sublimation approach that have helped improve the sensitivity and robustness of this method.[7,12] Although airbrush and sublimation have been widely used in MALDI imaging, matrix application with an automated sprayer is growing rapidly. Here, the MALDI matrix application is controlled robotically to provide a uniform and reproducible matrix layers.[1,4,7,13−16] Most robotic sprayers allow for tuning of the solvent spraying temperature, solvent flow rate, the velocity of the matrix spraying nozzle, and the number of spraying passes that affect the desired matrix density and crystal sizes.[14,17]

In effort to correctly address one's experimental goals, the MALDI matrix application method must be carefully considered. For example, in untargeted spatial metabolomics experiments, extraction and detection of the maximum number of endogenous molecules are ideal, but a balance must be struck to ensure that spatial information remains preserved (i.e., minimize analyte delocalization).[18,19] In the case of using a robotic sprayer, there are general guidelines regarding the influence individual parameters has on the resulting matrix film. Increasing the temperature at which the matrix solvent is applied to the sample, for example, will reduce the droplet size and generate small matrix crystals. Conversely, increasing the solvent flow rate and/or lowering the spray velocity can provide more wet conditions that facilitate higher analyte extraction.[17] To date, there are no specific approaches that guide optimal matrix application conditions for any one experiment when using an automated spraying device. Typical optimization strategies use sequential iterations that consider one variable at a time and neglect the effect one parameter has on the other. This approach to matrix application can be very time-consuming, and it may result in nonoptimal conditions because the whole experimental space was not systematically explored. To overcome these issues, we propose to use the response surface methodology (RSM).[20−22] This is a widely used optimization strategy in analytical chemistry,[20] where
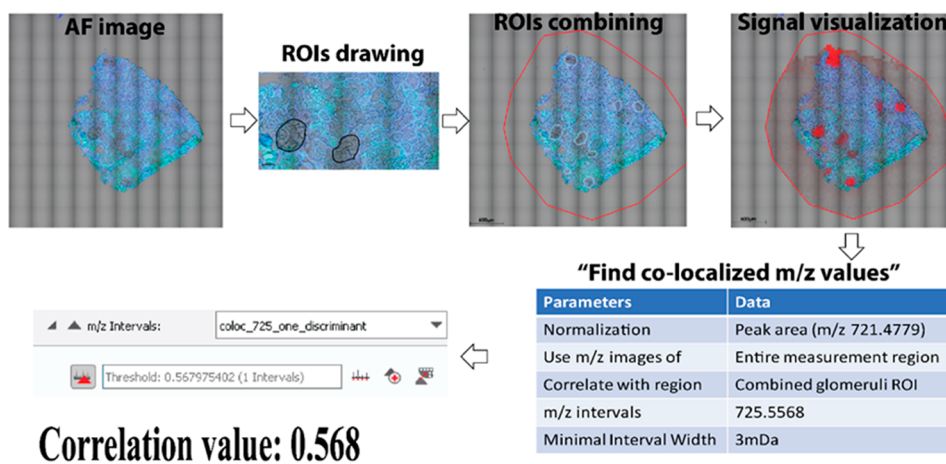
Figure 1. Workflow to determine signal delocalization using the SCiLS software. The autofluorescence image was used to determine the location of each glomerulus within the kidney tissue section, and each outlined glomeruli was then combined into a single ROI. Then the "Find Co-localized m/z values" function within SCiLS was ran to determine the correlation of m/z species, with the spectra normalized to m/z 721.4779 (a nonglomerulus marker), with the combined ROI. After this processing was done, we determined the correlation value of m/z 725.5568 (a characteristic glomerulus marker) with our ROI by manually adjusting the slider until our species of interest was included in the m/z interval list.

predictive mathematical models based on experimental data are created to optimize a chosen response. For example, in MALDI untargeted metabolomics analyses, this approach has been used for optimizing automated data acquisition parameters or ion transmission voltages and laser ablation parameters.[21,22]

Here, we developed an experimental approach for optimizing MALDI matrix spraying conditions to minimize analyte delocalization and simultaneously maximize the number of detected lipids in MALDI-FTICR-MSI analysis of frozen human kidney biopsies. By testing 32 combinations of MALDI matrix spraying parameters with an automated spraying device, we were able to model, using RSM, the effect each of the spraying parameters had on the delocalization of endogenous molecules and the ability to detect and annotate lipid species. This method can also be employed for other MALDI-MSI applications, types of samples, and matrix application strategies.

METHODS

Preparation of Human Kidney Biopsy Samples for MALDI-MSI. Fresh frozen human kidney biopsy tissue (18-gauge) was taken from a nephrectomy sample donated by the University of Michigan. The sample was mounted on a cryomicrotome chuck by freezing a small droplet of water that was delivered by a Pasteur pipet, and then sectioned (10 μm; CryoStar NX70, Thermo Fisher) using both a blade and specimen temperature of −15 °C. Sections were thaw-mounted onto indium tin oxide (ITO)-coated glass slides (Bruker Daltonics), in the sample configuration illustrated in Figure S1.

Tissue Autofluorescence Imaging. Tissue autofluorescence images used for overlaying with MALDI images were captured prior to MALDI matrix application. Autofluorescence images were acquired using a Zeiss 710 confocal microscope and a W plain-Apochromat 20× objective. Tissue sections were excited with 405 and 490 nm laser wavelengths and corresponding emission wavelengths were collected from 404 to 488 nm and 495−720 nm, respectively, for analysis.[23] Using the tile scan function in ZEN 2.3 SP1 software (Zeiss), several 303.6 μm × 303.6 μm images were stitched over different areas

on the slides to acquire mosaic images of whole tissue sections. Since, such large area mosaic acquisition takes time, z stack imaging of the 10 μm thick tissue sections was avoided by adjusting the pinhole size to an equivalent of 4.63 airy units. The pinhole adjustments allowed acquisition of image information above and below the focal plane. All microscopy images were analyzed using the ZEN image analysis software (Zeiss).

MALDI Matrix Application. A TM-Sprayer (model M3; HTX Technologies) was used for all MALDI matrix applications. In all 32 experiments, the concentration of DHB matrix was 40 mg/mL, while spraying parameters and solvent composition were varied according to the experimental design (Table 1). Furthermore, a N_2 pressure of 10 psi, a track spacing of 3 mm, and the distance between the nozzle and a sample of 40 mm were maintained for preparation of all samples.

MALDI-MSI Analysis. MSI was performed on a 15 T MALDI-FTICR-MS (Bruker Daltonics) equipped with a SmartBeam II laser source (355 nm, 2 kHz) in positive ion mode using 200 shots/pixel (2 kHz) and a 50 μm pitch between pixels. FTICR-MS, externally calibrated using ESI-Low Concentration Tuning Mix (Agilent), was operated to collect m/z 250−2000 using a 577 ms transient that translated to a mass resolving power of ~170,000 at m/z 400. For all 32 MALDI-MSI experiments, the ion transfer and analyzer parameters remained constant based on optimizing the system using the ESI source to allow maximal transmission and detections of signals m/z 600−900. Due to different matrix amounts across the different samples, the laser power was tuned for each experiment, so that the TIC was maintained for each experiment (~1 × 10^{10}).

Quantifying Co-Localization. SCiLS software (Bruker Daltonics) was used to assist in quantifying colocalization; see Figure 1 for a detailed workflow. Briefly, the autofluorescence image was used as a template for determining regions of interests (ROI), which in this case is each glomerulus within the kidney tissue section that were combined into a single ROI. Using SCiLS, we ran the "co-localized m/z values" analysis against the ROI, as illustrated at Figure 1. As a result, we could determine m/z intervals based on each colocalization factor

(Pearson's correlation coefficient) of a selected ion (i.e., m/z 721.4779).

Quantifying the Number of Detected Lipids. MALDI-FTICR-MS imaging data imported into the SCiLS software (SQLite format) was transformed to the imzML format using the "Export to METASPACE" tool, with spectra restriction using only the m/z intervals of the initially imported peaks. The resulting imzML and ibd files were then uploaded to METASPACE (https://metaspace2020.eu), Figure S2.[24] The data was annotated against the SwissLipids database[25] with an FDR of 20%, Figure S3. Lipid species that demonstrated localization predominantly in the off-sample region were manually removed from the list, and the resulting numbers of lipid annotations were used for RSM analysis (Figure S4).

Experimental Design and Statistical Analysis. The experimental design was used as an efficient tool for simultaneous determination of the effects of multiple factors and their interactions. Experiments were conducted using a central composite design (CCD) with 32 experimental points to investigate linear, quadratic, and cross-product effects of five factors (spraying parameters), each varied at five levels. The experimental design containing considered levels of variables and their actual values (in brackets) is shown in Table 1. In this design, the central point is replicated six times (experiments 27−32), so that standard deviation between analyses can be calculated (this is necessary for generating the model). Experiments were performed in random order to minimize systematic errors. The data obtained were analyzed by a response surface regression (RSREG) method to fit the second-order polynomial equation:

$$Y = b_0 + \sum_{i=1}^{k} b_i X_i + \sum_{i=1}^{k} b_{ii} X_i^2 + \sum_{i}^{i<j} \sum_{j} b_{ij} X_i X_j \tag{1}$$

where Y is the dependent variable (response variable), x_i and x_j are the independent variables (factors), b_0, b_i, b_{ii}, and b_{ij} are regression coefficients of the applied model. The Fisher's exact test was used to determine model adequacy, and the Student's distribution test was applied to evaluate the significance of the coefficients− this permitted evaluation to determine if all observed variables have a statistically significant effect on analyzed outputs. The coefficients of the response function and their statistical significance were evaluated by the least-squares method with the MATLAB software (The MathWorks, Matick, MA, USA). Only the significant terms ($p \leq 0.05$) were considered for the final model. Response surfaces plots were obtained using the fitted model, by keeping independent variables at a constant value while changing the other two variables.

RESULTS AND DISCUSSION

Optimizing Spraying Parameters for Minimizing Delocalization. In order to quantifying delocalization we utilized two molecular signals. First, we used m/z 725.5568, annotated as a sphingomyelin (SM; d34:1), which was previously associated with the kidney glomeruli.[26] Our light microscopy data confirmed colocalization of this signal predominantly within the glomerular region in all of our data sets as well. Second, we used m/z 721.4779, annotated as phosphatidic acid (PA; 36:3), which was detected everywhere outside of the glomeruli. Our spectral images were normalized to this signal in effort to gain a more complete insight into the diffusion of other species in- and out- of the glomeruli, Figure

1. Using this approach, we found the colocalization of m/z 725.5568 with the ROI of the glomeruli varied from 0.046 to 0.630 (Table 1, Y_1) − representative images can be seen in Figure 2.
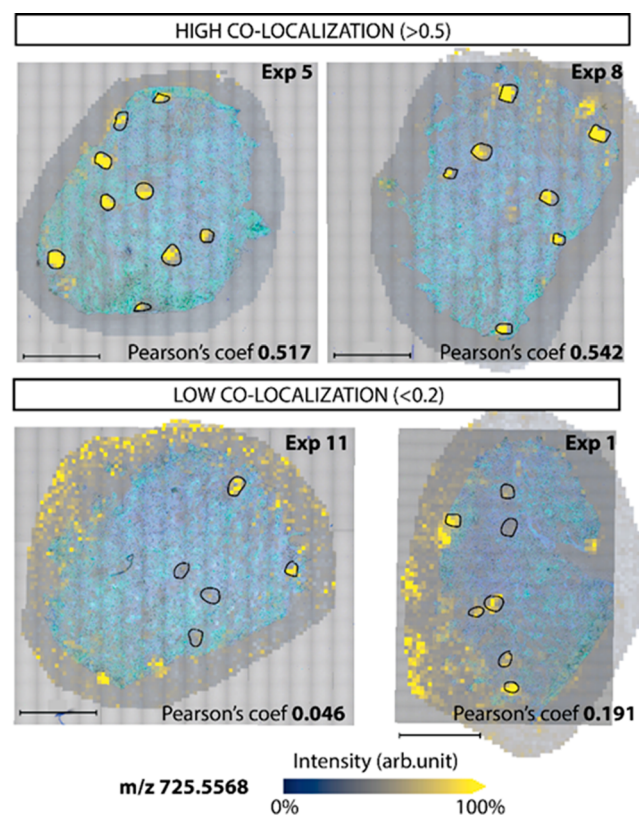

Figure 2. Representative MALDI-MS ion images of m/z 725.5568 with high and low colocalization to the glomeruli within the human kidney biopsy tissue sections (upper and lower images, respectively). The glomeruli are outlined in black. Note that low colocalization implies high delocalization and vice versa. Scale bars are 1 mm.

These results, as tabulated in Table 1, were fit to a second-order regression model, and after elimination of the insignificant coefficients, the following regression model was obtained:

$$Y_1 = 0.4125 + 0.0379X_1 - 0.0651X_2 - 0.045X_4$$
$$- 0.0427X_4^2 - 0.0345X_5^2 - 0.0431X_2X_4 \tag{2}$$

To illustrate how each of these variables affects molecular delocalization, this model was plotted in Figure 3. According to this model, the flow rate (X_2) has a large linear negative impact on species colocalization. In other words, an increase in flow rate increases molecular delocalization (Figure 3a). This makes sense given the faster the flow rate, the larger the droplets that will be sprayed onto the sample, and thus a larger surface area of solvent that will impact the sample during matrix application. Increase in temperature (X_1) is the only factor that has a linear positive effect on minimizing delocalization (Figure 3a), as elevated temperatures cause application of dryer solvent conditions that lead to smaller droplets of matrix solution hitting the sample. Molecular delocalization has a quadratic dependence on the number of spray cycles (X_4) and methanol concentration (X_5) in our model (Figure 3b), where we found an optimal MeOH concentration and number of
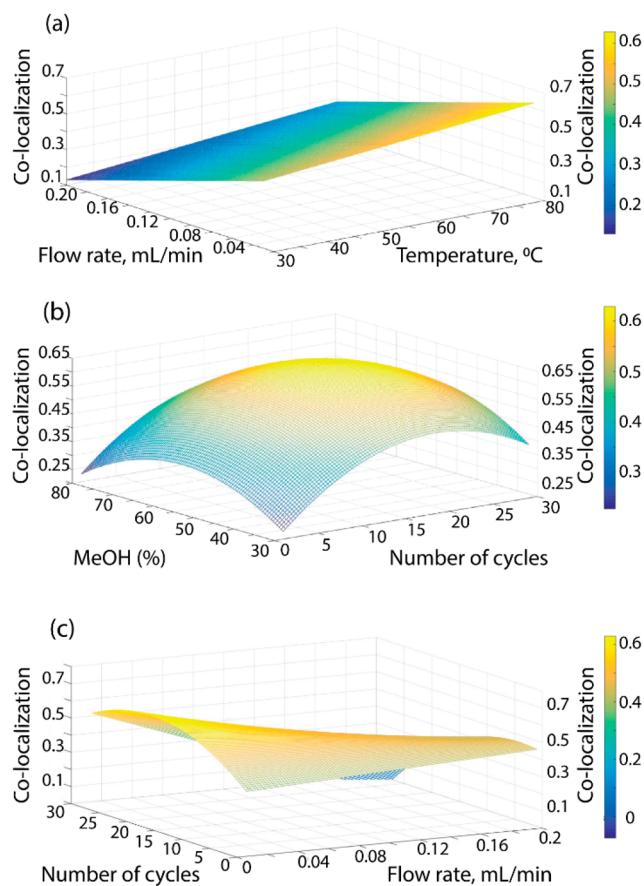
Figure 3. Response surfaces of significant experimental factors based on the model in eq 2. These plots illustrate the effects of different spraying parameters for matrix application on the colocalization of MSI signal m/z 725.5568 to the glomerular region within the kidney biopsy tissue. (a) Effect of flow rate and sprayer head nozzle temperature; fixed variables: $X_4 = 0.5$; $X_5 = 0$. (b) Effect of MeOH concentration and the number of spraying cycles; fixed variables: $X_1 = 2$; $X_2 = -2$. (c) Effect of the number of spraying cycles and flow rate have on the colocalization; fixed variables: $X_1 = 2$; $X_5 = 0$.

spray cycles to be 55% and 18, respectively. This model also suggests the negative interdependency between the flow rate (X_2) and a number of cycles (X_4), Figure 3c. In fact, at high flow rates decreasing the number of cycles will reduce delocalization, but at low flow rates, the dependence follows the opposite trend. Moreover, if the number of cycles is minimized then changing the flow rate barely affects delocalization, while at a high number of cycles, increasing the flow rate will significantly delocalize the observed signal. Interestingly, the spray velocity (X_3), which is the rate at which the sprayer head moves across the sample, seems to have no effect on this model, although one can assume that slower spraying will lead to droplets pooling and hence larger extraction volumes. Notably, the relatively moderate step size (50 μm) and moderate laser focus (≈ 25 μm) used for generating ion images can also explain why this effect was not observed as significant.

Overall, this model reveals that the optimal parameters for minimal signal delocalization for DHB application onto human kidney biopsy tissues sectioned at 10 μm thickness is 55% MeOH, 18 spray cycles, 80 °C, and a 0.01 mL/min flow rate, which provided the highest Pearson's correlation of 0.630. One can hypothesize that a lower flow rate and a higher

temperature can lead to even lower delocalization, but in our experience such parameters resulted in inconsistent spray (due to rapid evaporation of the solvent at the nozzle tip). Accordingly, these parameters were intentionally not included in our model.

Optimization of Spraying Parameters for To Evaluate Sensitivity. We used the number of molecular annotations we were able to attain for a sample in METASPACE as an indicator of our measurement sensitivity. A previous study on optimizing MALDI conditions utilized an alternative approach, where the number of mass spectral features above a given signal-to-noise threshold was used an indicator of measurement sensitivity.[7] The key advantage of using our META-SPACE approach is that the annotation numbers are comparable between different tissue sections and protocols, as they are attained with an internal quality control (i.e., based on a false discovery rate approach).[24] Further, METASPACE annotations account only for signals that correspond to known, curated, endogenous molecules, and thus exclude unknown signals that are possibly associated with sample preparation artifacts. Finally, METASPACE combines signals corresponding to naturally occurring isotopes into one annotation, by matching the isotope abundance data with the monoisotopic species detection.

We used the default METASPACE tolerance of 3 ppm. Our data was acquired in positive polarity, and we considered the default set of ion adducts in METASPACE to be $[M + H]^+$, $[M+K]^+$, and $[M + Na]^+$. METASPACE not only uses accurate mass, but also the isotopic pattern intensities (correlated to the theoretically predicted intensities), as well as other measures (measure of spatial chaos, measure of colocalization of the isotopic ion images) that are all integrated into one MSM measure.[24] We selected a 20% FDR in effort to attain higher molecular coverage of annotated species. While 20% FDR is higher than the default value in METASPACE (10% FDR[24]), we wanted to increase our number of annotations in effort to capture those annotations that capture delocalized or leaked metabolites. Worth noting is that METASPACE annotations at 20% FDR are still more reliable than using accurate mass matching alone, which achieves 25% FDR, at best.[24]

Across our experiments, the numbers of annotated lipid species in METASPACE ranged between 11 and 333 (Table 1, Y_2). Similar to as done above, we quantified the impact of the spraying parameters on MALDI sensitivity (i.e., based on the numbers of annotated lipids). The following regression model was obtained after eliminating insignificant coefficients:

$$Y_2 = 144.88 - 32.53X_2 + 20.18X_3 + 25.44X_4 + 4X_5$$
$$+ 13.34X_5^2 - 36.55X_2X_4 + 27X_2X_5 + 21.73X_3X_4 \tag{3}$$

eq 3 is plotted in Figure 4, which illustrates how the different spraying parameters affected MALDI sensitivity. For example, these results suggest that there is a positive linear impact of spraying velocity (X_3) on the number of annotations in METASPACE (Figure 4a). Further, Figure 4b reveals that the maximal number of annotations was achieved in minimal MeOH concentration and flow rate (note, a maximum of function when both parameters are at a minimum). Figure 4c illustrates that by increasing the flow rate with a high number of cycles significantly decreases the number of detected lipids, in comparison to using a lower number of cycles. Accordingly,
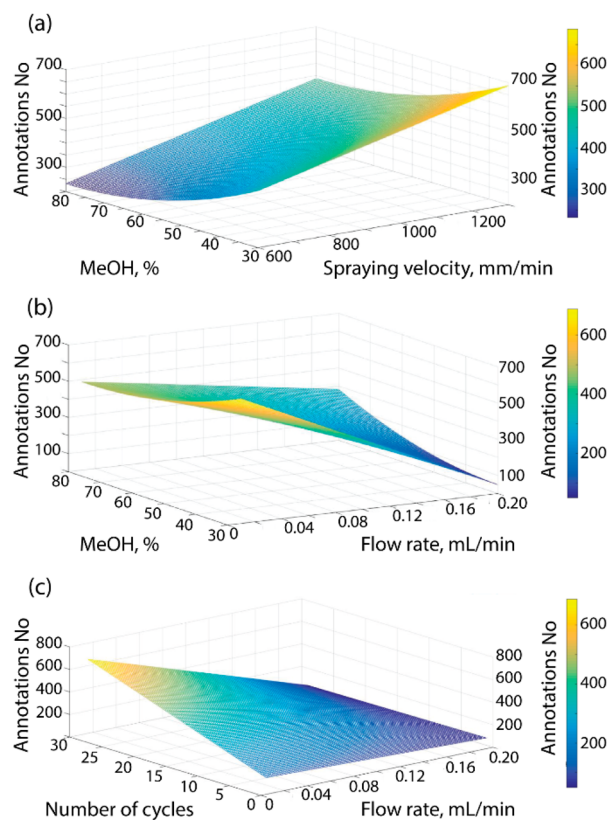
Figure 4. Response surfaces of significant experimental factors based on the model in eq 3, showing the effects of spraying parameters onto the sensitivity measured as the number of lipid annotations in METASPACE. (a) Effect of MeOH concentration and spraying velocity; fixed variables: $X_2 = -2$; $X_4 = 2$. (b) Effect of MeOH concentration and flow rate; fixed variables: $X_3 = 2$; $X_4 = 2$. (c) Effect of the number of spraying cycles and flow rate; fixed variables: $X_3 = 2$; $X_5 = -2$.

the maximum response is observed using the maximal number of cycles and minimal flow rate.

Interestingly, our model suggest that the maximal number of annotations requires rather extreme application parameters: 30% MeOH, 29 spray cycles, a flow rate of 0.01 mL/min, and a spraying velocity of 1300 mm/min. Given that the highest spraying velocity and lowest flow rate tested gave the most annotations, our results show that the "wettest" conditions do not necessarily provide the best sensitivity. This could be due to the fact that using the lowest spray velocity and highest flow rate would result in more matrix being applied to the sample, which in turn could suppress detection of endogenous molecules. More likely analyte extraction is promoted using an increased amount of water in the matrix solvent, rather than delivering a larger amount of solvent per sample surface area.

The representative mass spectra in Figure 5 illustrate how signal in the lipid range (m/z 700−850) increased from severely suboptimal, to suboptimal, to nearly optimal MALDI matrix spraying conditions (experiments 24, 30, and 5, respectively, in Table 1). These results show good agreement with the number of annotated species attainable by using the SwissLipid DB in METASPACE. Specifically, the total number of MS peaks in m/z 700−850 range with a S/N threshold of 4 and a relative ion abundance threshold of 0.01% were 384, 504, and 540 for the severely suboptimal, suboptimal, and near-
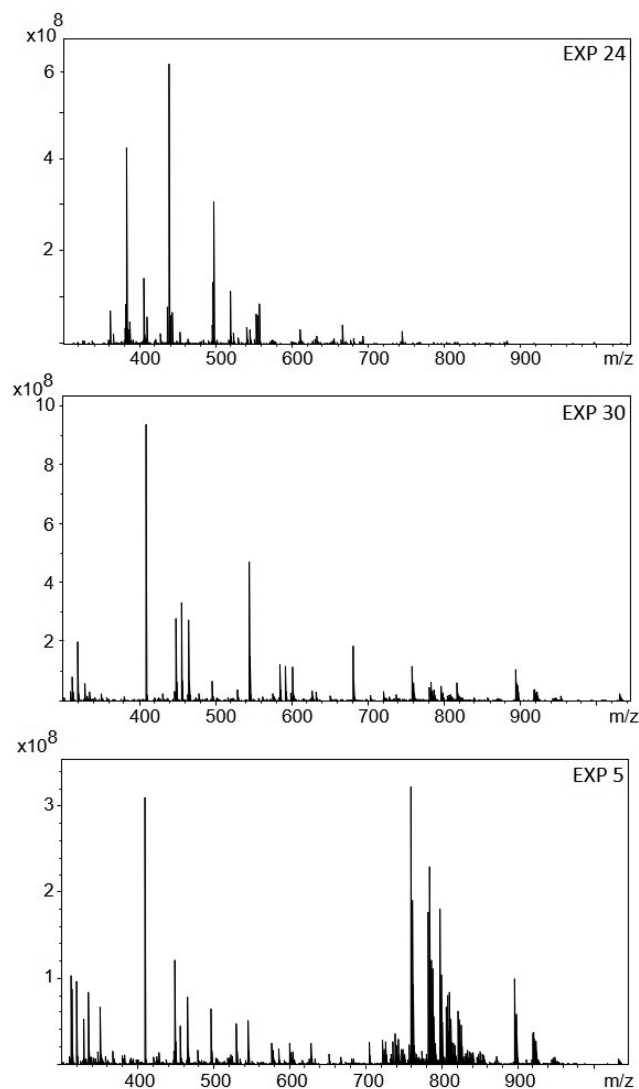
Figure 5. Representative MALDI-MS spectra (m/z 300−1,000) using severely suboptimal (experiment 24), suboptimal (experiment 30), and near optimal (experiment 5) matrix spraying protocols.

optimal conditions, respectively, which provided 11, 126, and 333 annotations in METASPACE, respectively.

Notably, our data shows that nozzle temperature (X_1)— within the range tested (30−80 °C)—was not a significant factor in the number of annotations attained from a sample. This was counterintuitive, as one would expect lower temperatures to produce bigger droplets and more "wet" conditions and, in turn, provide higher analyte extraction. We retested this, replicating the temperature extremes from the model (i.e., 30 and 80 °C, the lowest and highest temperature, respectively), and kept all other parameters at 0 coded values. These results showed that the variance in the number of annotations between the two temperatures was only 6%, which is lower than the CV for this entire experiment (17%). Thus, this confirms our surprising finding that for the considered samples and matrix application protocol, the spraying temperature is an insignificant parameter for MALDI sensitivity.

These results illustrate the nonlinear relationships between the spraying parameters and the achieved sensitivity. Thus, we caution about using single-parameter optimization approaches, where one parameter is optimized at a time, as these results

can be misleading in predicting the optimal matrix application parameters. Presumably, this complexity is because the number of detected species is influenced by the extraction efficiency, which depends on many factors like the endogenous abundance of all species, the solvent composition, the volume of the deposited solvent droplet, the temperature of extraction, and the analyte's cocrystallization ability with a given matrix.[27] As such, changing each of these parameters will influence the optimal conditions for each of the other parameters.

Balancing between Spatial Delocalization and Sensitivity. The optimal matrix application method would ideally minimize analyte delocalization within the sample while maximizing sensitivity. For MALDI-MSI, delocalization is problematic; therefore, matrix application conditions should be chosen that minimize delocalization, even if they provide optimal MALDI sensitivity. Accordingly, we picked where the correlation of m/z 725.5568 and the glomeruli ROI had a Pearson correlation coefficient >0.6. Our models suggested that the choice of spray velocity (1300 mm/min) and temperature (80 °C) were straightforward to determine, because the former factor is insignificant for molecular delocalization, while the latter factor was insignificant for the number of annotations. Notably, both models from Figures 3 and 4 had an optimal flow rate of 0.01 mL/min. Conversely, the factors that showed quite different optimal values between these two models were the MeOH concentration and the number of application cycles. The compiled effects of these factors on normalized outcomes is depicted in Figure 6. As
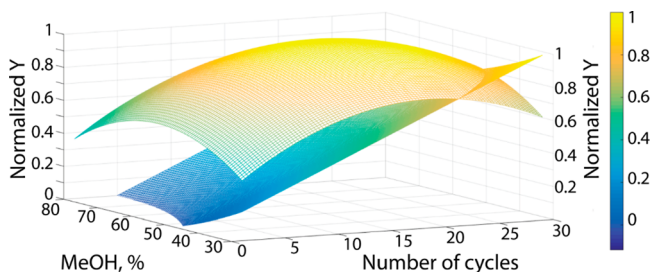
Figure 6. Response surfaces of the effect of number of spraying cycles and MeOH concentration on normalized outputs. Normalized outputs were calculated by dividing models with the maximum output values, specifically eq 2 by 0.63 and eq 3 by 688; fixed variables: $X_1= 2$; $X_2= -2$; $X_3= 2$.

such, if we want to maximize the number of annotations with the prerequisite that the Pearson correlation coefficient is >0.6, according to our response surface model, the number of cycles should be 24 with a 46.5% MeOH concentration, which predicts upward of 442 molecular annotations from these kidney biopsy samples.

CONCLUSION

In this paper, we demonstrated how the utilization of the response surface methodology provided optimized MALDI-MSI matrix application parameters for human kidney biopsy tissue samples. We used human kidney tissue biopsies in this study because we faced a real-world application challenge as part of the US NIH Kidney Precision Medicine Program, where in part our goal is to develop optimized protocols for analyzing these tissue types from patients. However, the powerfulness of this method is that it can also be employed for other MALDI-MSI applications, molecular classes, samples

types, and sample preparation protocols, where it is especially valuable for automated devices. Note, the purpose of this manuscript is not to provide a universal model for matrix spraying, but rather it is to demonstrate how MALDI imaging outputs can be maximized by using this experimental approach and creating models. For our RSM, we considered two critical criteria for determining optimal matrix spraying conditions, namely spatial delocalization of endogenous molecules and analytical sensitivity, where we developed unbiased quantification approaches to achieve both criteria. Even though we manually filtered out annotated species with intensities predominantly outside of the tissue in this work, an automated filtration strategy based on deep learning recognition of off-sample images was recently implemented in METASPACE. Thus, employing our approach for future work will be faster and completely unbiased. Combining with other experimental optimization approaches, like that of ion transmission voltage optimization[21] and/or automated data acquisition optimization,[22] our approach using RSM for MALDI matrix application optimization can be valuable for attaining the most ideal spatial and chemical information from future MALDI-MSI analyses.

Compliance with Ethical Standards. Prior to the initiation of the study, an IRB approval for study of human participants was obtained at University of Michigan. The consent form included all of the elements required by the OHPR, FDA, state local and institutional regulations, as well as any additional elements relevant to the specific study situation as required by ethical regulations and guidelines.

ASSOCIATED CONTENT

Supporting Information

The Supporting Information is available free of charge at https://pubs.acs.org/doi/10.1021/jasms.9b00074.

Step-by-step protocol and important notes for optimizing the HTX TM-spraying parameters using the RSM, containing (Table S1) coded and actual values of factors used in the experimental design, (Figure S1) organization of tissue biopsy sections on slides together with HTX TM-sprayer conditions used for each section, (Figure S2) example METASPACE webpage that shows the uploading process, (Figure S3) example METASPACE webpage that displays putative molecular annotations and corresponding ion images, and (Figure S4) examples of endogenous and off-tissue annotations by METASPACE (PDF)

AUTHOR INFORMATION

Corresponding Author

Christopher R. Anderton − *Environmental Molecular Sciences Laboratory, Pacific Northwest National Laboratory, Richland, Washington 99352, United States; Center for Renal Precision Medicine, University of Texas Health-San Antonio, San Antonio, Texas 78284, United States;* orcid.org/0000-0002-6170-1033; Email: christopher.anderton@pnnl.gov

Authors

Dušan Veličković − *Environmental Molecular Sciences Laboratory, Pacific Northwest National Laboratory, Richland, Washington 99352, United States*

Guanshi Zhang − *Center for Renal Precision Medicine, University of Texas Health-San Antonio, San Antonio, Texas 78284, United States*

Dejan Bezbradica − *Department of Biochemical Engineering and Biotechnology, Faculty of Technology and Metallurgy, University of Belgrade, Belgrade 11000, Serbia*

Arunima Bhattacharjee − *Environmental Molecular Sciences Laboratory, Pacific Northwest National Laboratory, Richland, Washington 99352, United States*

Ljiljana Paša-Tolić − *Environmental Molecular Sciences Laboratory, Pacific Northwest National Laboratory, Richland, Washington 99352, United States*

Kumar Sharma − *Center for Renal Precision Medicine, University of Texas Health-San Antonio, San Antonio, Texas 78284, United States*

Theodore Alexandrov − *Structural and Computational Biology Unit, European Molecular Biology Laboratory, Heidelberg 69117, Germany; Skaggs School of Pharmacy and Pharmaceutical Sciences, University of California San Diego, La Jolla, California 92093, United States*

KPMP Consortium − *Kidney Precision Medicine Project (KPMP), National Institute of Diabetes and Digestive and Kidney Diseases, National Institutes of Health, Bethesda, Maryland 20892, United States*

Complete contact information is available at:
https://pubs.acs.org/10.1021/jasms.9b00074

Notes

The authors declare no competing financial interest.

■ REFERENCES

(1) Gemperline, E.; Rawson, S.; Li, L. J. Optimization and Comparison of Multiple MALDI Matrix Application Methods for Small Molecule Mass Spectrometric Imaging. *Anal. Chem.* **2014**, *86*, 10030−10035.

(2) Velickovic, D.; Agtuca, B. J.; Stopka, S. A.; Vertes, A.; Koppenaal, D. W.; Paga-Tolic, L.; et al. Observed metabolic asymmetry within soybean root nodules reflects unexpected complexity in rhizobacteria-legume metabolite exchange. *ISME J.* **2018**, *12*, 2335−2338.

(3) Velickovic, D.; Chu, R. K.; Carrell, A. A.; Thomas, M.; Pasa-Tolic, L.; Weston, D. J.; et al. Multimodal MSI in Conjunction with Broad Coverage Spatially Resolved MS2 Increases Confidence in Both Molecular Identification and Localization. *Anal. Chem.* **2018**, *90*, 702−707.

(4) Velickovic, D.; Ropartz, D.; Guillon, F.; Saulnier, L.; Rogniaux, H. New insights into the structural and spatial variability of cell-wall polysaccharides during wheat grain development, as revealed through MALDI mass spectrometry imaging. *J. Exp. Bot.* **2014**, *65*, 2079−2091.

(5) Caprioli, R. M.; Farmer, T. B.; Gile, J. Molecular imaging of biological samples: Localization of peptides and proteins using MALDI-TOF MS. *Anal. Chem.* **1997**, *69*, 4751−4760.

(6) Chughtai, K.; Heeren, R. M. A. Mass Spectrometric Imaging for Biomedical Tissue Analysis. *Chem. Rev.* **2010**, *110*, 3237−3277.

(7) Huizing, L. R. S.; Ellis, S. R.; Beulen, B.W.A.M.M.; Barré, F. P. Y.; Kwant, P. B.; Vreeken, R. J.; et al. Development and evaluation of matrix application techniques for high throughput mass spectrometry imaging of tissues in the clinic. *Clinical Mass Spectrometry.* **2019**, *12*, 7−15.

(8) Warren, A. D.; Mitchell, D. J.; Gates, P. J. Methodologies for the airbrush application of MALDI matrices. *Eur. J. Mass Spectrom.* **2018**, *24*, 89−95.

(9) Li, B.; Comi, T. J.; Si, T.; Dunham, S. J. B.; Sweedler, J. V. A one-step matrix application method for MALDI mass spectrometry imaging of bacterial colony biofilms. *J. Mass Spectrom.* **2016**, *51*, 1030−1035.

(10) Hankin, J. A.; Barkley, R. M.; Murphy, R. C. Sublimation as a method of matrix application for mass spectrometric imaging. *J. Am. Soc. Mass Spectrom.* **2007**, *18*, 1646−1652.

(11) Rešetar Maslov, D.; Svirkova, A.; Allmaier, G.; Marchetti-Deschamann, M.; Kraljevic Pavelic, S. Optimization of MALDI-TOF mass spectrometry imaging for the visualization and comparison of peptide distributions in dry-cured ham muscle fibers. *Food Chem.* **2019**, *283*, 275−286.

(12) Fernandez, R.; Garate, J.; Martin-Saiz, L.; Galetich, I.; Fernandez, J. A. Matrix Sublimation Device for MALDI Mass Spectrometry Imaging. *Anal. Chem.* **2019**, *91*, 803−807.

(13) Ly, A., R, Longuespee, R., Casadonte, P., Wandernoth, K., Schwamborn, C., Bollwein, et al.: Site-to-Site Reproducibility and Spatial Resolution in MALDI-MSI of Peptides from Formalin-Fixed Paraffin-Embedded Samples. *Proteomics: Clin. Appl. 13,* (**2019**).1800029

(14) Iloro, I.; Bueno, A.; Calvo, J.; Urreta, H.; Elortza, F. Langartech: A Custom-Made MALDI Matrix Sprayer for MALDI Imaging Mass Spectrometry. *Jala-J. Lab Autom.* **2016**, *21*, 260−267.

(15) Anderton, C. R.; Chu, R. K.; Tolic, N.; Creissen, A.; Pasa-Tolic, L. Utilizing a Robotic Sprayer for High Lateral and Mass Resolution MALDI FT-ICR MSI of Microbial Cultures. *J. Am. Soc. Mass Spectrom.* **2016**, *27*, 556−559.

(16) Bradshaw, R.; Denison, N.; Francese, S. Implementation of MALDI MS profiling and imaging methods for the analysis of real crime scene fingermarks. *Analyst* **2017**, *142*, 1581−1590.

(17) Creissen, A., Demonstration of matrix deposition optimization. *Improving protein detection and reduction of analyte delocalization.* Technical Note # 31, HTXImaging, 2015.

(18) Li, B.; Zhang, Y.; Ge, J. Y.; Liu, K. H.; Li, P. Sample preparation for mass spectrometry imaging of leaf tissues: a case study on analyte delocalization. *Anal. Bioanal. Chem.* **2018**, *410*, 7449−7456.

(19) Anderson, D. M. G.; Floyd, K. A.; Barnes, S.; Clark, J. M.; Clark, J. I.; Mchaourab, H.; et al. A method to prevent protein delocalization in imaging mass spectrometry of non-adherent tissues: application to small vertebrate lens imaging. *Anal. Bioanal. Chem.* **2015**, *407*, 2311−2320.

(20) Bezerra, M. A.; Santelli, R. E.; Oliveira, E. P.; Villar, L. S.; Escaleira, L. A. Response surface methodology (RSM) as a tool for optimization in analytical chemistry. *Talanta* **2008**, *76*, 965−977.

(21) Ferey, J.; Marguet, F.; Laquerriere, A.; Marret, S.; Schmitz-Afonso, I.; Bekri, S. A new optimization strategy for MALDI FTICR MS tissue analysis for untargeted metabolomics using experimental design and data modeling. *Anal. Bioanal. Chem.* **2019**, *411*, 3891.

(22) Zhang, L.; Borror, C. M.; Sandrin, T. R. A designed experiments approach to optimization of automated data acquisition during characterization of bacteria with MALDI-TOF mass spectrometry. *PLoS One* **2014**, *9*, No. e92720.

(23) Patterson, N. H.; Tuck, M.; Lewis, A.; Kaushansky, A.; Norris, J. L.; Van de Plas, R.; et al. Next Generation Histology-Directed Imaging Mass Spectrometry Driven by Autofluorescence Microscopy. *Anal. Chem.* **2018**, *90*, 12404−12413.

(24) Palmer, A.; Phapale, P.; Chernyavsky, I.; Lavigne, R.; Fay, D.; Tarasov, A.; et al. FDR-controlled metabolite annotation for high-resolution imaging mass spectrometry. *Nat. Methods* **2017**, *14*, 57−60.

(25) Aimo, L.; Liechti, R.; Hyka-Nouspikel, N.; Niknejad, A.; Gleizes, A.; Gotz, L.; et al. The SwissLipids knowledgebase for lipid biology. *Bioinformatics* **2015**, *31*, 2860−2866.

(26) Miyamoto, S.; Hsu, C. C.; Hamm, G.; Darshi, M.; Diamond-Stanic, M.; Decleves, A. E.; et al. Mass Spectrometry Imaging Reveals Elevated Glomerular ATP/AMP in Diabetes/obesity and Identifies Sphingomyelin as a Possible Mediator. *EBioMedicine.* **2016**, *7*, 121−134.

(27) Quiason, C. M.; Shahidi-Latham, S. K. Imaging MALDI MS of Dosed Brain Tissues Utilizing an Alternative Analyte Pre-extraction Approach. *J. Am. Soc. Mass Spectrom.* **2015**, *26*, 967−973.